

SPIO-labeled ⁹⁰Y microspheres permit accurate quantification of macroscopic intra-hepatic biodistribution

Weiguo Li^{1,2}, Zhuoli Zhang¹, Yang Guo¹, Jodi Nicolai¹, Reed A. Omary¹, and Andrew C. Larson¹

¹Radiology, Northwestern University, Chicago, Illinois, United States, ²Research Resource Center, University of Illinois at Chicago, Chicago, Illinois, United States

Target audience Interventional radiologist for liver cancer therapy.

Purpose Radioembolization with Yttrium-90 (⁹⁰Y) microspheres is a promising form of intra-arterial therapy for liver tumors [1]. Visualization of ⁹⁰Y microsphere biodistribution using conventional radiologic modalities is challenging [2]. Labeling ⁹⁰Y microspheres with SPIOs offers the potential to use MRI for visualization. Feasibility studies demonstrated that SPIO-labeled radioembolization microspheres permit qualitative visualization of microsphere biodistribution following transcatheter delivery to the liver [3]. However, optimization of the amount of SPIO material included within these glass microspheres may be critical. The objective of this study was to characterize the relationship between ⁹⁰Y microsphere SPIO content and associated MR imaging properties and to validate that quantitative R₂* measurements permit *in vivo* quantification of SPIO-labeled microsphere biodistribution.

Methods Phantom: We constructed 32 agarose gel phantoms for each of four different microsphere compositions (2%, 5%, 10%, and 20% SPIO (%-by-mass)). Agarose gel was placed within 15 mm ID NMR tubes along with 0, 0.25, 0.5, 1.0, 2.0, 4.0, 8.0, or 16.0 mg/ml samples of SPIO-labeled microspheres for each composition of ⁹⁰Y microsphere to form a homogeneous distribution of the microspheres.

Rat model: All the experiments are approved by the Institutional Animal Care and Use Committee. Male Sprague-Dawley rats weighing 200–350 g were used. The rats were anaesthetized by inhalation of 2% vaporized isoflurane. Each rat was catheterized through hepatic portal vein with a rat portal vein catheter (Charles River, Wilmington, MA). After catheterization, MR imaging was performed before and after administration of microspheres. 5 mg samples of microspheres containing 2 % SPIO were administered with two injections and two saline flushes for each injection through the catheter. After MRI, rats were euthanized, and livers were harvested and fixed using 10% buffered formalin for histological analysis (hematoxylin and eosin (H&E) staining).

MRI: All studies were performed using a 7.0 T 30 cm bore Bruker ClinScan MRI scanner (Bruker Biospin, Ettlingen, Germany) with a) 75mm Quad Transceiver rat coil, b) isoflurane anesthesia system, body temperature control and monitoring system for vital signs, and c) MRI-compatible small animal gating system (SA Instruments, NY) to permit free-breathing acquisitions for pre- and post-procedural MRI measurements. The phantoms are positioned at the center of magnet. Careful manual shimming was performed before R₂* measurement. Quantitative R₂* measurements were obtained by using a multiple-gradient-echo (mGRE) sequence with TR/TEs = 200/2.6, 5.7, 8.8, 11.9 ms; 30° flip angle, 1-mm section thickness, 65-mm field of view, 192 × 192 matrix, readout bandwidth of 360 Hz/pixel. For rat imaging, all the scans were synchronized with the respiratory cycle to minimize motion artifacts. Quantitative R₂* measurements were performed using mGRE sequence with TR/TEs = 200/2.6, 5.7, 8.8, 11.9 ms; 30° flip angle, FOV = 65 × 60 mm²; matrix = 192 × 192; slice thickness = 0.7 mm, readout bandwidth of 360 Hz/pixel.

Data Analysis: Image post-processing was performed offline by using Matlab software (The Math Works, Natick, MA). R₂* maps were calculated using the nonlinear Levenberg-Marquardt algorithm to fit the monoexponential decay component: $S_{TE_i} = S_0 \cdot \exp(-R_2^* \cdot TE_i)$, where S_{TE_i} is the MR signal intensity at echo time TE_i, S₀ is the MR signal intensity at echo time 0, and TE_i is the echo time. Regions of interest (ROI) that encompassed each concentration of microspheres were drawn on the R₂* map obtained in each microsphere composition phantom. Color-coded R₂* maps of the rat liver was overlaid on the T₂* weighted images to highlight the voxel-wise changes following the intra-hepatic microsphere delivery.

Results T₂* weighted images of microsphere phantom showed a decreasing signal intensity with increase in microsphere concentration (Fig.1a). For microspheres with 5, 10, and 20% iron compositions, the measured R₂*s dropped when concentrations produced R₂* values beyond an upper limit threshold (about 750 sec⁻¹; Fig. 1b). A linear relationship was found across all seven concentrations of 2% ⁹⁰Y microspheres (blue line Fig.1b). Histological analysis results (Fig.2) verified microsphere deposits in liver vessels. Coronal T₂* weighted images with color-coded overlays depicting voxel-wise estimates of intra-hepatic microsphere concentration are shown in Fig. 3. Representative examples are shown pre- and post-infusion (Figs. 3a, and b) of the microspheres.

Discussion and Conclusion The clinical ability to quantify intra-hepatic ⁹⁰Y microsphere deposition would provide enormous benefits permitting dose optimization to maximize tumor kill while limiting toxic effects on normal liver tissues. SPIO-labeled ⁹⁰Y microspheres offer the potential to use MRI to detect *in vivo* biodistribution; however, the strong magnetic susceptibility effects of these SPIO-labeled microspheres can rapidly reduce signal below the noise floor complicating rigorous quantification. In current study, given the measured approximately 500 sec⁻¹ R₂* value at the concentration of 16 mg/ml for 2% microspheres, higher concentrations of the microsphere could also be quantitatively detected for ⁹⁰Y microspheres with 2% of SPIO. ⁹⁰Y microspheres doped with 2% SPIO have the potential to be used for *in vivo* to quantification of macroscopic intra-hepatic biodistribution. SPIO-labeled ⁹⁰Y microspheres offer the potential to use MRI R₂* maps to quantitatively depict *in vivo* biodistribution. With the current study we have demonstrated the potential to optimize SPIO content for future studies intended to quantify microsphere concentrations delivered to liver tumors *in vivo*.

Reference [1] Salem R *et al.* Int J Radiat Oncol Biol Phys. 2006. [2] Salem R *et al.* Tech Vasc Interv Radiol. [3] Gupta T *et al.* Radiology. 2008.

Acknowledgements: The authors wish to acknowledge the support of NIH grant RO1 CA134719, and SIR Foundation Pilot Grant.

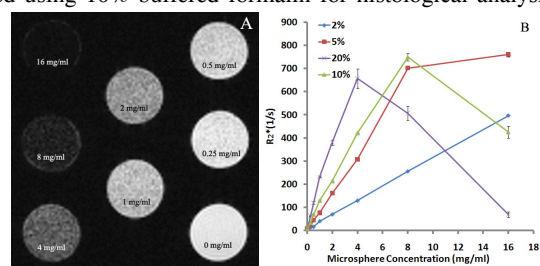


Fig.1 a) T₂* weighted images of 5% ⁹⁰Y microsphere phantoms (TR/TE =200/5.7 ms). b) Transverse relaxation rates R₂* versus ⁹⁰Y concentration for 4 different compositions

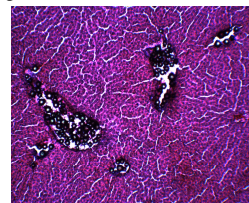


Fig.2 H&E staining of liver tissue with microspheres.

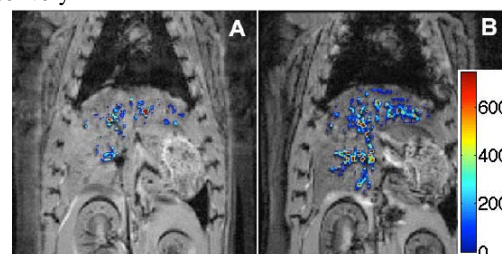


Fig.3. Coronal MGRE images with color-coded overlays depicting voxel-wise estimates of intra-hepatic microsphere concentration. A) pre-infusion; B) post-infusion. Colorbar unit: sec⁻¹